

## **Seasonal climate sensitivity to the sea-ice cover in an intermediate complexity AGCM**

*Ivana Herceg Bulić<sup>1</sup> and Čedo Branković<sup>2</sup>*

<sup>1</sup> Department of Geophysics, Faculty of Science, University of Zagreb, Zagreb, Croatia

<sup>2</sup> Croatian Meteorological and Hydrological Service, Zagreb, Croatia

*Received 5 September 2005, in final form 27 February 2006*

The sensitivity of the atmospheric circulation to a different specification of sea-ice temperature and its seasonal cycle is analysed from the 50-year long integrations with SPEEDY, an intermediate complexity atmospheric general circulation model (AGCM). This impact is inferred from the difference between model atmospheric states obtained with and without the inclusion of the thermodynamic effects of sea ice. The two experiments with sea ice were made – the first one used climatological monthly mean temperatures for sea ice (derived from ERA-15 data), whereas in the second experiment the sea-ice temperature was determined by a thermodynamic model embedded into the SPEEDY code.

It is shown that the thermodynamic model tends to amplify the seasonal cycle of temperature. In the boreal winter, the inclusion of the thermodynamic model for sea-ice temperature leads to a general cooling of the model atmosphere at high latitudes (when compared with the experiment with climatological sea ice), associated with the reduction in geopotential heights and the strengthening of zonal winds. It also reduces the extent and amount of cloud cover in the mid- and high latitudes. Atmospheric cooling could be directly linked to the increased sea-ice seasonal cycle, because the increased albedo over sea ice reduces incoming solar radiation and further stabilises already cold air. Some of the changes induced by sea ice extend throughout the whole depth of the model atmosphere and could be linked directly to strong meridional differential temperature gradients. In addition, some seasonally varying symmetry between the Northern and the Southern Hemisphere is also found.

In summer when the receding sea ice is included in model integration, the opposite effects are seen: differential temperature gradients are of the opposite sign, the atmosphere is warmed thus effecting a reduction in zonal winds and an increase in cloudiness. These effects are stronger in amplitude than those associated with the maximum winter extent of sea ice, suggesting that ocean heat flux from the ice-free water together with increased solar radiation and convection bear a strong mark on the model atmosphere.

*Keywords:* seasonal climate sensitivity, thermodynamic effects of sea-ice, intermediate complexity AGCM

## 1. Introduction

Variability of the global atmosphere on time scales beyond deterministic predictability is primarily driven by slowly varying forcings at the lower boundary. Sea surface temperature (SST) is certainly the main contributing factor; however, the effects of, for example, sea ice, soil moisture, snow cover, land surface albedo and land surface temperature on this externally caused variability are far from being negligible (*e.g.* Palmer and Anderson, 1994). Interactions and feedbacks between the atmosphere and underlying surface may cause changes in the amplitude of atmospheric monthly to seasonal scale variability (*e.g.* Molteni et al., 1993; Palmer, 1993). Internal atmospheric variability (or atmospheric chaotic properties) also plays a role, in particular in regime transitions, though it has limited predictability.

Sea ice is an important component of the climate system and a sensitive indicator of climate change. It affects global climate by influencing the thermohaline circulation and by changing the location of storm tracks. For example, Honda et al. (1996) modelled the influence of the Sea of Okhotsk sea ice on large-scale atmospheric circulation and found a remote response in the form of tropospheric stationary wave emanating from the Sea of Okhotsk towards North America. Because sea ice acts as a barrier between the oceans and the atmosphere, it strongly influences transfers of moisture, heat and momentum. Changes to sea ice cover have impacts on surface albedo, surface turbulent heat fluxes, surface wind drag and upper-ocean stratification. These changes reveal a strong seasonal variability, however, they are modulated by atmospheric conditions as well (*e.g.* Deser et al., 2000; Fang and Wallace, 1994; Gloersen, 1995; Maslanik et al., 1999).

Murray and Simmonds (1995) studied response of the northern winter climate to the reduction in the Arctic sea ice. They showed that the speed and intensity of cyclonic systems north of 45 °N decreased significantly, but found little overall change in the positioning of the major storm tracks. They also found that the decrease in sea ice concentration causes a monotonic but non-linear warming in the lower troposphere and a weakening and southward contraction of the mid-latitude westerlies. In contrast, Parkinson et al. (2001) found that the warming in the lower troposphere is linear since the surface air temperature increases linearly as the concentration of sea ice decreases. Alexander et al. (2004) investigated local atmospheric response on realistic Arctic sea ice anomalies during winter. Their model results showed that the Arctic sea-ice reduction is accompanied with a near-surface warming, enhanced precipitation and below-normal sea level pressure.

Some model experiments that considered extremes in sea ice conditions pointed out that the removal of all sea ice in the Northern Hemisphere would cause an increase in low-level Arctic temperatures (*e.g.* Newson, 1973; Warshaw and Rapp, 1973; Royer et al., 1990). In addition, in most of these studies, a reduced mean sea-level pressure and weakened mid-latitude westerlies were

found. The ambiguous nature of sea-level pressure response to sea-ice reduction is found in simulations for both Northern and Southern Hemisphere circulations (Herman and Johnson, 1978; Mitchell and Hills, 1986; Mitchell and Senior, 1989). In their study on sensitivity of the South Hemisphere circulation to sea ice concentration, Simmonds and Budd (1991) found that decreased sea-ice concentration is associated with a warming of the troposphere and a weakening of westerlies.

Observations and climate modelling studies show that sea ice considerably impacts variability of local climate. According to Wu et al. (2004) sea ice anomalies in the Greenland and Barents Seas display important feedback impacts on local atmospheric boundary layer in terms of both thermodynamic and dynamic processes. They also found that the increased concentration of sea ice stabilises the overlaying layer between 850 and 700 hPa. Furthermore, cooling associated with increased albedo and the sea ice insulation effect during the winters with abundant sea ice lead to shallow surface high pressure. Agnew (1993) found a general weakening of the Aleutian and Icelandic lows for severe sea-ice conditions, suggesting a reduced surface heating as a possible cause. This may have an impact on large-scale circulation patterns, like for example, the North Atlantic Oscillation (NAO). Kahl (1990) showed that sea ice influences boundary layer temperature along the Alaskan Arctic through the development of low-level temperature inversion. Tjernström et al. (2005) have found recently that most atmospheric parameters in the Arctic boundary layer simulated by six state-of-the-art regional climate models agree reasonably well with observations. This is certainly encouraging bearing in mind possible impacts of climate change on the Arctic region in general and on sea ice in particular.

The purpose of this study is to examine how a different specification of sea-ice temperature and its seasonal cycle affect the seasonal mean state of the model atmosphere. This is realised by using an atmospheric general circulation model (AGCM) of intermediate complexity in the 50-year long integrations. Furthermore, one of the goals is to find out whether some regularity in the atmospheric response to sea ice forcing exists in both hemispheres. The robustness of our results was attained by running the model over a relatively long period of time. Within the framework of experimental design, this effectively corresponds to a relative large ensemble with comparably shorter time integrations. The model and experiments are described in the next section. The results are shown and discussed in section 3. In section 4, summary and concluding remarks are given.

## 2. Model and experiments

The model used in this study is a simplified atmospheric general circulation model nicknamed SPEEDY (from »Simplified Parameterizations, primitive-Equation DYNamics«), with 8 vertical levels and a triangular truncation

of horizontal spectral fields at total wave number 30 (T30–L8). An earlier version of the model with 5 vertical layers is described in details in Molteni (2003) together with its climatology and variability. One of the main features of SPEEDY is its computational efficiency. SPEEDY is based on a spectral dynamical core developed at the GFDL<sup>1</sup> (see Held and Suarez, 1994). It is a hydrostatic,  $\sigma$ -coordinate, spectral transform model in the vorticity-divergence form described by Bourke (1974), with semi-implicit treatment of gravity waves. The parameterised processes include short- and long-wave radiation, large-scale condensation, convection, surface fluxes of momentum, heat and moisture, and vertical diffusion. Land and ice temperature anomalies are determined by a simple one-layer thermodynamic model.

Molteni (2003) discussed SPEEDY response to tropical and extratropical SST anomalies for a model version with five vertical layers. He found that the model is capable to simulate atmospheric flow realistically, especially during the boreal winter. Furthermore, different ranges of atmospheric variability were reproduced in SPEEDY simulations, albeit with smaller amplitude than that obtained from the observations. The 7-layer version of the model is significantly improved compared with the 5-layer version. The comparison of the 7-layer model for the period 1952–2001 with the NCEP/NCAR<sup>2</sup> reanalysis (Kalnay et al., 1996) confirms the ability of SPEEDY to simulate reasonably well the forced and internal components of the atmospheric interdecadal variability, and to estimate the response of the atmospheric circulation to the well documented SST trends in the tropical oceans (Bracco et al., 2004). As the model used in this study has 8 layers in the vertical, it is hoped that the improved vertical resolution improves model climatology. In our experiments the model top was set at 50 hPa and the time step was 40 minutes.

The analysis performed in this work is based on the two 50-year SPEEDY simulations. In the first (control) experiment, denoted as SSTC, the forcing at the model lower boundary is specified by climatological SST with its annual cycle and by climatological sea ice cover with its own annual cycle. Both climatological SST and sea-ice datasets are in the form of monthly averages obtained from a long time series of observational data and provided from the ERA-15<sup>3</sup> dataset (Gibson et al., 1997). In this case, surface temperature values over sea ice points are taken from the SST dataset, in which, based on temperature itself, the distinction between sea ice points and open-sea points is not obvious. Since the boundary forcing in this experiment is being repeated

---

<sup>1</sup> Geophysical Fluid Dynamics Laboratory, University of Princeton, Princeton, New Jersey, U.S.A.

<sup>2</sup> National Oceanic and Atmospheric Administration, National Weather Service, National Centers for Environmental Prediction, Camp Springs, Maryland/ National Center for Atmospheric Research, Boulder, Colorado, U.S.A.

<sup>3</sup> European Centre for Medium-Range Weather Forecasts' re-analysis

via the SST annual cycle (and modulated by the sea-ice extension) throughout the model integration, the only seasonal-scale variability comes from the monthly varying SSTs. The usage of sea ice in SSTC is essentially reduced for the definition of surface albedo, which in turn affects net surface radiation.

The second experiment, denoted as ICE\_SSTC, differs from the first one in the computation of surface temperature over sea ice. In contrast to SSTC, surface temperature in ICE\_SSTC is computed in the same way as over model land points, *i.e.* from the expression for the net heat flux into the surface, which includes net radiation and sensible and latent heat fluxes. The equation for surface temperature over sea ice could be written in the following form

$$c\Delta z \frac{\partial T}{\partial t} = F - c\Delta z \cdot \lambda (T - T_{\text{clim}}),$$

where  $\Delta z$  is the thickness of the ice layer (1.8 m),  $c$  is the heat capacity of ice ( $1.93 \cdot 10^6 \text{ J m}^{-3}$ ),  $F$  is the net heat flux into the surface,  $\lambda$  is the relaxation time (20 days) for temperature anomalies over sea ice  $T$ , and  $T_{\text{clim}}$  is prescribed climatological temperature of sea ice computed from ERA-15. Thus, boundary forcing in ICE\_SSTC is different from that in SSTC in the part related to sea ice, whereas for open-sea points it remains identical to that in SSTC. It is important to point out that in many polar regions sea ice never melts in summer implying that the effect of sea ice is still »felt« in the nearby ice-free water. This has an important implication for the model physics in the sea-ice bordering zones: heat fluxes interact with and are modulated by predefined surface temperature values from the SST dataset. The difference between the ICE\_SSTC and SSTC experiments indicates the thermodynamical impact of sea ice on the model integration.

Apart from seasonal-mean values, the experiments also differ in the spectrum of variability for sea-ice temperature. The SSTC only includes the seasonal cycle, while the ICE\_SSTC also has intra-seasonal variability. Since heat fluxes are non-linear, the mean heat flux in the ICE\_SSTC is different from the heat flux that would be obtained by fixing the seasonal-mean value. This effect is strong in neutral or unstable conditions, while is less important in the stable conditions prevailing over the polar regions.

As mentioned above, in both experiments the climatological monthly averages of SST and sea-ice fraction are specified repeatedly at the lower boundary over the 50-year period. This implies that boundary forcing is essentially »fixed«, *i.e.* there is no interannual variability at the lower boundary. The only year-to-year *atmospheric* variability comes primarily from model's internal dynamics (and interactions and feedbacks between model dynamics and physics). Bracco et al. (2004) found in their experiments with SPEEDY that in the extratropics the ratio between externally forced signal and internally generated variability (or noise) is less than 0.2. This indicates that the external forcing is overwhelmed by model's internal variability. Therefore, for

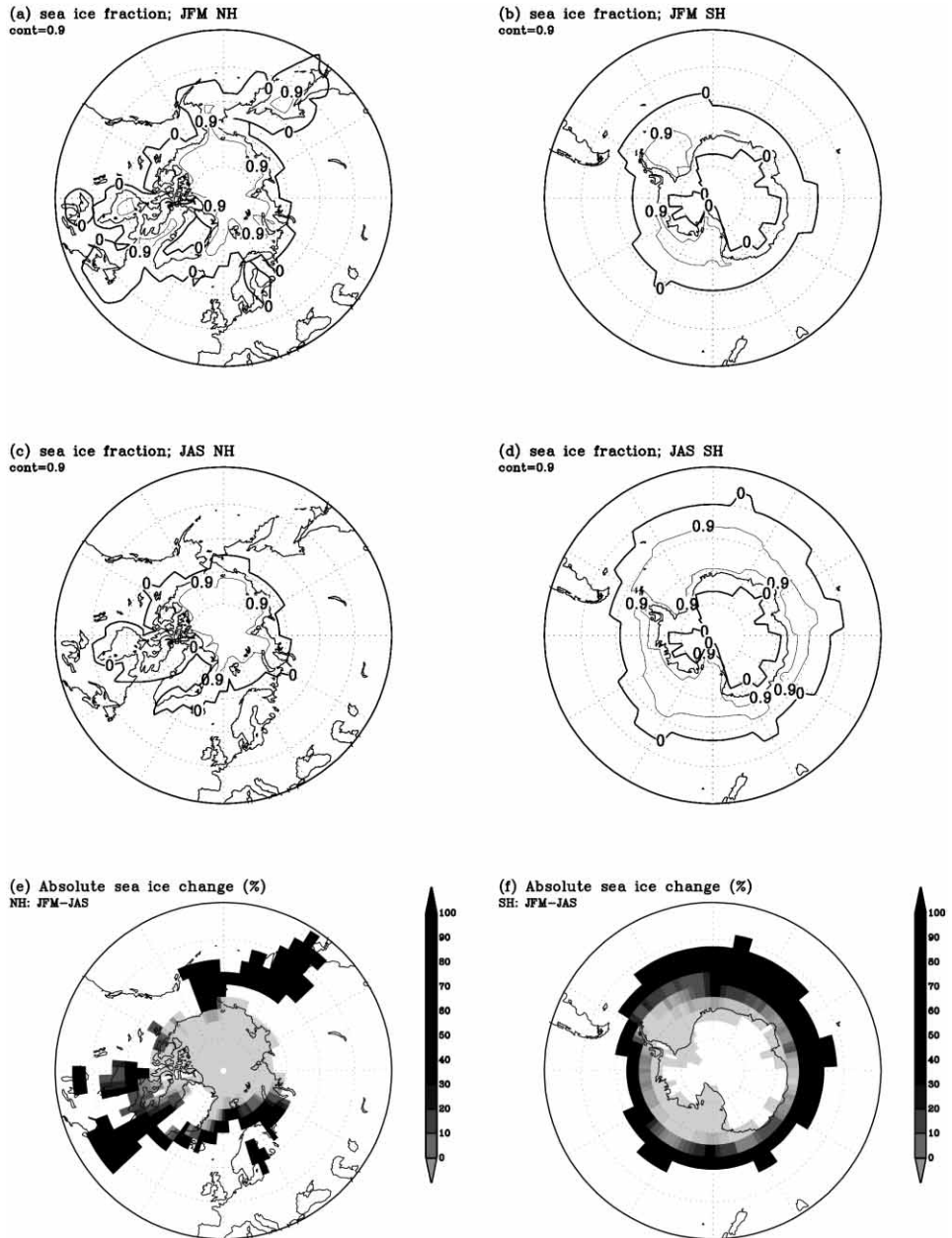


**Figure 1.** Sea ice fraction (between 0 and 1) for: a) Northern Hemisphere JFM, b) Southern Hemisphere JFM, c) Northern Hemisphere JAS, d) Southern Hemisphere JAS, e) absolute sea ice change (%) in the Northern Hemisphere, and f) absolute sea ice change (%) in the Southern Hemisphere. Contours in a) to d) at 0.0 and 0.9.

the purpose of our experiments' analysis, we may assume that internally caused differences in the model runs »mimic« the model (year-to-year) variability that would normally be imposed from slight changes in either initial and/or boundary conditions. Of course, this assumption is not strictly true, however, it is valid within the framework of our experiments. Consequently, although only two long model runs were at our disposal, it might be assumed that effectively we deal with the two 50-member ensembles of one-year long integrations. Thus, it could be claimed that our study is based on statistically representative samples. A simple analysis, based primarily on seasonal averages for the two seasons is carried out – for JFM (January, February, March) and JAS (July, August, September).

Before discussing the model results, we briefly present the seasonally averaged distribution of sea ice used in both experiments. As expected, there is a large difference in the distribution of sea ice between the Southern and the Northern Hemisphere polar regions (Fig. 1). The seasonal sea-ice fraction that varies between 0 and 1 clearly outlines the boundary between ice-covered and ice-free parts (the marginal ice zone). In the Northern Hemisphere during JFM, sea ice covers the Arctic Ocean, and large parts of the Greenland Sea, Barents Sea and the Sea of Okhotsk. In JAS, the marginal ice zone moves poleward and the sea-ice cover is restricted to the northern part of the Arctic Ocean and the Greenland Sea.

The Southern Hemisphere polar regions are affected by a much larger seasonal variation in sea-ice cover than the northern counterpart in both spatial extension and amplitude. In the southern summer (JFM), sea ice is confined to the region poleward of approximately 60 °S (Fig. 1b), whereas in the southern winter (JAS) the sea-ice distribution extends to 50 °S (Fig. 1d). Irrespective of season, the distribution of sea ice around Antarctica is more symmetric and more uniform than in the Arctic.

Fig. 1e and 1f show the percentage change of the sea-ice cover between its extreme extensions as defined by the JFM and JAS seasons. The dark shading indicates the complete sea ice melt in the summer season. In the Northern Hemisphere, it covers the northern Pacific and northern Atlantic bordering seas as well as some inland waters (like the Baltic Sea, Hudson Bay and the Great Lakes). A large part of the Arctic Ocean remains covered by sea ice throughout the year (light shading). In the Southern Hemisphere, sea ice completely melts in the zonal strip around 60 °S, and the maximum latitudinal change is in the southern Atlantic.

### 3. Results

#### 3.1. Global fields

As mentioned above, the results are discussed in terms of seasonally mean atmospheric variables, averaged over the 50-year period. We refer to these

averages as model climate, and to the SSTC experiment as the control run. The thermodynamic effects of sea ice on model climatology are assessed from seasonally mean differences between the ICE\_SSTC and SSTC simulations and our main interest is the response of the model global circulation to the imposed surface forcing.

(i) *Temperature*

Since the effects of sea ice are introduced in SPEEDY through (surface) temperature field, we first discuss the model response in terms of the upper-air temperature. The JFM and JAS seasonal averages of the 850 hPa temperature in SSTC (no thermodynamic effect of sea ice) represent the expected climatological seasonal temperature distribution with lowest temperatures in the winter polar regions of both hemispheres (Fig. 2a and 2b). In the northern winter, the coldest regions are Siberia and the Canadian Arctic with temperatures exceeding  $-30$  and  $-25$  °C respectively; in the Southern Hemisphere, the JAS 850 hPa temperature exceeds  $-40$  °C over Antarctica. However, some of these very cold values over Antarctica are, to a certain

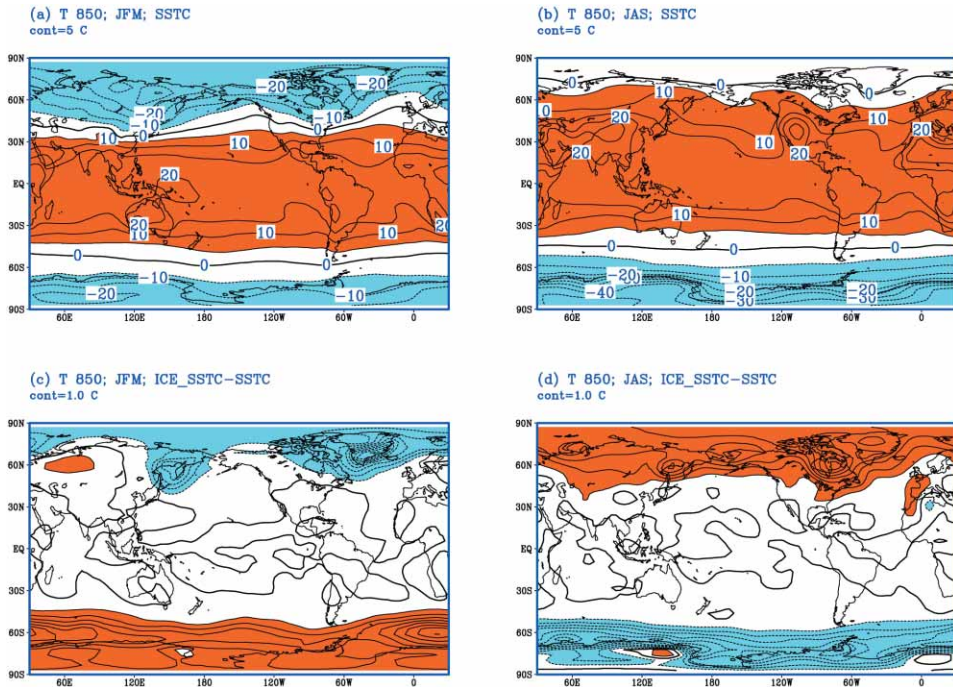


**Figure 2.** Temperature at 850 hPa for: a) SSTC full field in JFM, b) SSTC full field in JAS, c) difference ICE\_SSTC minus SSTC in JFM, and d) difference ICE\_SSTC minus SSTC in JAS. Contours every 5 °C in a) and b), and every 1 °C in c) and d). Positive values dark shaded (solid), negative values light shaded (dashed).

extent, fictitious because of the extrapolation of model results to below-ground pressure levels in post-processing. In the Southern Hemisphere mid and high latitudes, the isotherms are nearly zonal because of a relative uniform longitudinal land/sea, and consequently, sea ice distribution (c.f. Fig. 1d). The strongest meridional temperature gradients are found in hemispheric winter seasons over the bordering regions between land and sea; however, these regions do not always coincide with the extension of sea ice.

The difference between ICE\_SSTC and SSTC experiments indicate that the impact of the sea ice thermodynamics on the lower troposphere temperature is confined mainly to high latitudes (Fig. 2c and 2d). The sign of differences clearly shows seasonal variation: negative differences in winter hemispheres, and positive differences in summer hemispheres. Since in both experiments the sea-ice coverage was identical, negative differences in Fig. 2c and 2d could be attributed to a contributing thermodynamical effect of the winter sea-ice to the low-level atmosphere cooling. This is strongly highlighted in the Southern Hemisphere, where negative differences closely coincide with the extent of sea ice (cf. Fig. 1d). In the Northern Hemisphere, similar response of the model is seen over the (closed) Sea of Okhotsk and the Canadian Arctic (the Labrador Sea and the Hudson Bay), *i.e.* the cooling effect is localised due to the stabilisation of the lower atmosphere. Relatively large amplitude of differences over Greenland and Antarctica could be again (at least partly) attributed to the model post-processing in the region of high orography. The low-level atmosphere cooling during winter (with more sea ice than in summer) is in agreement with some previous studies (*e.g.* Kahl, 1990; Wu et al., 2004).

In the Southern Hemisphere summer (Fig. 2c), when the extent of sea ice is much reduced in comparison to the winter season (Fig. 1b), the impact is strongest in the southern Atlantic with positive differences reaching +8 °C. Figure 1f clearly indicates that this is the region with largest variation in the sea-ice extent. It could be argued that the thermal equilibrium over sea ice in the ICE\_SSTC experiment is biased away from the one found in the SSTC experiment, *i.e.* as defined in ERA-15 data. Such a change in the thermal equilibrium between the two experiments might be linked to the change in the surface heat flux. Indeed, the JFM difference in the surface heat flux between ICE\_SSTC and SSTC experiments indicates an increase along the narrow strip of sea-ice melt (cf. dark shaded areas in Fig. 1f) reaching more than 30 Wm<sup>-2</sup> in the southern Atlantic (not shown). It seems therefore as if the model in the ICE\_SSTC experiment tends to overestimate the summer differences in the surface heat flux that spread from the surface over much wider area into the atmosphere above, as indicated by Fig. 2c.

In the Northern Hemisphere summer, positive differences extend over many continental areas. This indicates the effect of warm continental temperatures induced by seasonal cycle in solar radiation that warms continents more quickly than the adjacent oceans because of their low heat capacity. However, the largest positive differences are found in the land-bordering

regions of the Sea of Okhotsk and in the Canadian Arctic pointing out to the (additional) effect of relative warm SSTs freed of sea ice. Positive differences over the Greenland Sea and parts of the Norwegian Sea could be attributed to a poleward shift of the marginal ice zone. As for the southern summer, an increase in the sensible heat flux over these regions is found (not shown).

The impact of the sea-ice thermodynamics on the temperature field extends to higher levels as well. For example, the pattern of winter cooling at 500 hPa is similar to that at 850 hPa, however, with considerably smaller amplitude (Fig. 3a and 3b; note the different contouring interval to that in Fig 2c and 2d). Similar is true for summer hemispheres' warming; however, though the amplitude of warming is reduced when compared to 850 hPa, its reduction is not as large as in winter hemispheres. This again indicates that the effects of warm continents and warm (ice-free) seas, by virtue of larger eddy diffusivity, are stronger and penetrate deeper in the atmosphere than the effects of winter cooling by sea ice (see also the discussion in section 3.2 below).

At 200 hPa, there is some similarity with cooling and heating differences at lower levels, albeit with a much reduced amplitude (Fig. 3c and 3d). In

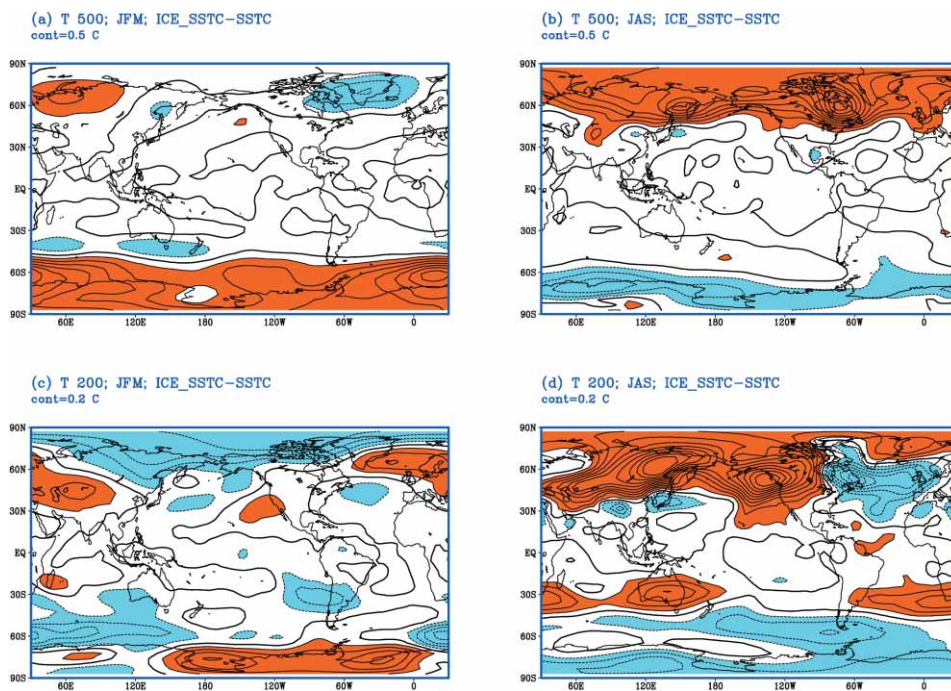


**Figure 3.** Temperature differences ICE\_SSTC minus SSTC for: a) 500 hPa in JFM, b) 500 hPa in JAS, c) 200 hPa in JFM, and d) 200 hPa in JAS. Contours every 0.5 °C in a) and b), and every 0.2 °C in c) and d). Shading as in Fig.2.

addition, although cooling (heating) dominates in the winter (summer) hemispheres, it is mixed with temperature differences of the opposite sign. This might indicate that, at high latitudes, the surface heat forcing does not penetrate deep into the upper troposphere, or that the thermal balance becomes affected by some other physical or/and dynamical processes.

(ii) *Geopotential height*

Similar to the temperature field, geopotential height differences between the ICE\_SSTC and SSTC experiments display seasonal regularity. For example, Fig. 4a and 4b shows that in the polar regions of both hemispheres, the winter (summer) 500 hPa differences are negative (positive). The locations of both positive and negative maxima generally coincide well with those for temperature shown in Figs. 2 and 3. In addition to these well-defined patterns and, in terms of amplitude relatively large model response in high latitudes, Fig. 4 also shows height differences of the opposite sign located away from high latitudes, in the direction of the equator. In the Northern Hemisphere winter, positive differences are seen over the northern Pacific and northern Atlantic thus forming dipole structures in the storm track regions. Similar pattern is found over the southern Pacific during JAS. Summer dipoles are weak in the Northern Hemisphere, but in the Southern Ocean marked negative differences are found alongside pronounced positive summer differences.

The geographical distribution of geopotential differences in both lower and upper troposphere is similar to that at 500 hPa (not shown), essentially indicating their barotropic structure. Of course, such a pattern in geopotential height differences has an effect on the changes in hemispheric winds (see the discussion below) that are induced primarily via horizontal (temperature) gradients. The amplitude of differences in the lower troposphere is weaker than that seen in Fig. 4; however, the amplitude of differences in the upper troposphere is larger in summer and about the same in winter when compared to that in Fig. 4. The latter points out that a relative strong surface and near

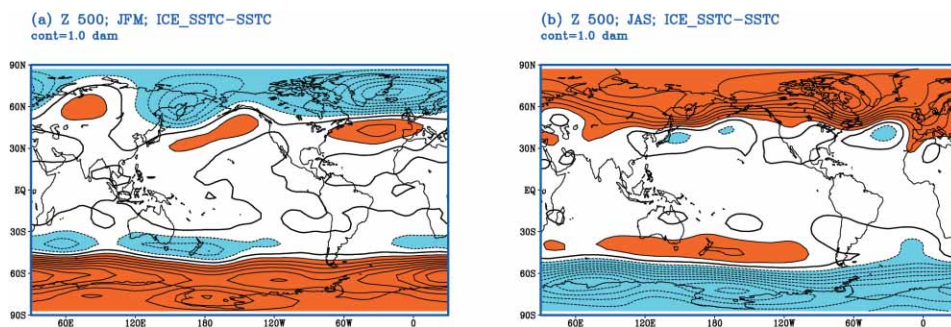


**Figure 4.** 500 hPa geopotential height differences ICE\_SSTC minus SSTC for: a) JFM, and b) JAS. Contours every 1 dam. Shading as in Fig.2.

surface warming in summer (either by heat flux due to the absence of sea ice cover or by heating from the continents, or by a combination of both) may cause that the low-level heat is conveyed to high altitudes. This is ultimately manifested as an increase of geopotential height as shown in Fig.4. The analysis of processes that might be responsible for such an energy transfer from the boundary to the upper troposphere is beyond the scope of this paper.

### (iii) Zonal wind

The main features of the 850-hPa climatological zonal wind ( $u$ -wind) are shown in Fig. 5a and 5b. In the mid-latitudes of both hemispheres the westerly winds prevail. In the northern winter they clearly indicate the Pacific and Atlantic storm tracks, which are considerably weakened during summer. In the southern hemisphere strong mid-latitude westerlies persist throughout the year («roaring forties»). Between these two belts of westerlies, in the tropical region there are easterlies, also known as trade winds over the oceans. Weak easterlies in the northern Pacific are a part of the winter Aleutian low system.

The difference between ICE\_SSTC and SSTC experiments (Fig. 5c and 5d) indicates a strengthening (weakening) of westerlies in both hemispheres dur-

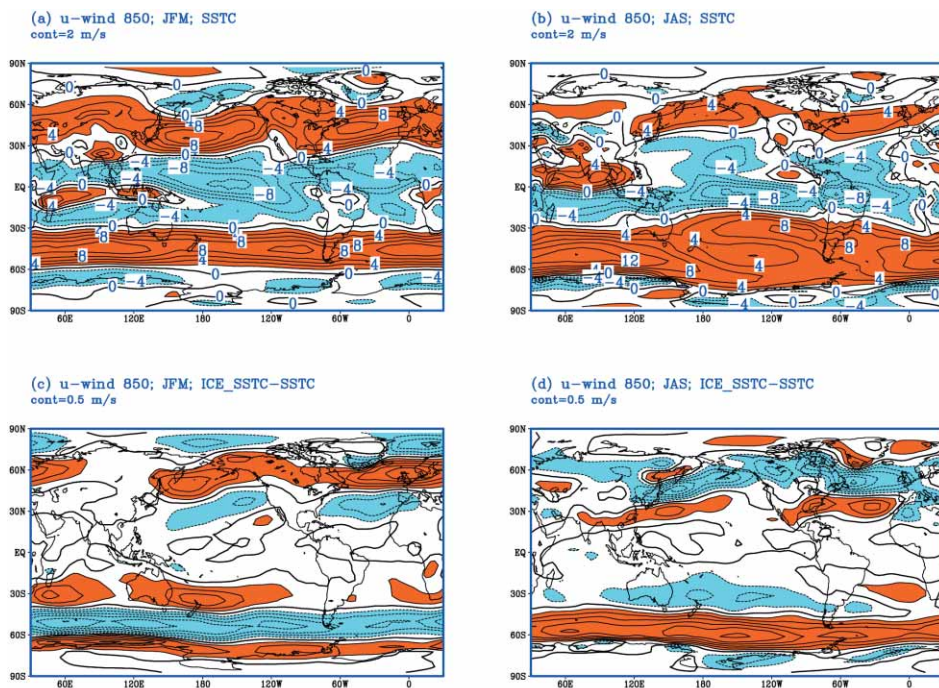


**Figure 5.** As Fig.2 but for 850 hPa  $u$ -wind. Contours every 2  $\text{ms}^{-1}$  in a) and b), and every 0.5  $\text{ms}^{-1}$  in c) and d).

ing the hemispheric winter (summer). This is consistent with the sign (direction) of the meridional differential temperature gradients shown in Fig. 2c and 2d: cooler temperatures to the left (right) of the wind direction cause an increase in the wind speed in the Northern (Southern) Hemisphere. Since, as discussed above, these differential temperature gradients are influenced by seasonal variations in sea ice, the variation of low-level winds might be indirectly linked to the sea ice annual cycle. This result agrees with the modelling studies of Newson (1973), Warshaw and Rapp (1973) and Royer et al. (1990) who found that the complete removal of sea ice in the Northern Hemisphere caused a weakening of the mid-latitude westerlies. Though the amplitude of wind differences (between 2.5 and 3  $\text{ms}^{-1}$  for both weakening and strengthening) is similar in both hemispheres, their spatial extension is much larger in the southern mid-latitudes. This can be attributed to the difference in the land/sea distribution between the two hemispheres, *i.e.* the nearly land-free belt at around 60 °S makes much smaller obstruction for the low-level southern westerlies than the continents of the Northern Hemisphere.

At upper levels, the pattern of the ICE\_SSTC minus SSTC wind differences is similar to that at 850 hPa, however with somewhat larger amplitude (not shown). The regions with cooling (warming) could be associated with the wind strengthening (weakening). This generally occurs throughout the depth of the model atmosphere and is consistent with the barotropic structure of temperature differences shown in Figs. 2 and 3. This will be further discussed in subsection 3.2 below.

#### (iv) Cloudiness

Clouds are important part of the climate system because they interact with the atmosphere in various ways. In case of our experiments, seasonal variation of the sea ice extent will, with most of its effects in high latitudes, influence clouds through changes in surface albedo (thus affecting solar radiation) and the ocean surface heat flux. Over sea ice, albedo is increased in comparison to ice-free water and therefore reduces the incoming solar radiation. In summer, the ocean heat flux from ice-free water is released into the atmosphere inducing an increased generation of clouds.

The climatological distribution of total cloud cover for the two seasons is displayed in Fig. 6a and 6b. In the tropics cloud cover is high and is associated with increased convective activity in intertropical convergence zones (ITCZs). The seasonal displacement of ITCZs is also evident; they are positioned to the south (north) of the equator during the JFM (JAS) season. In the subtropics, low cloud cover indicates areas of strong air subsidence. The cloudiness increases in the mid-latitudes of both hemispheres with the maxima corresponding to the storm tracks regions. It is again reduced at high latitudes poleward of approximately 70° where a generally weak subsidence prevails due to a very cold underlying surface.

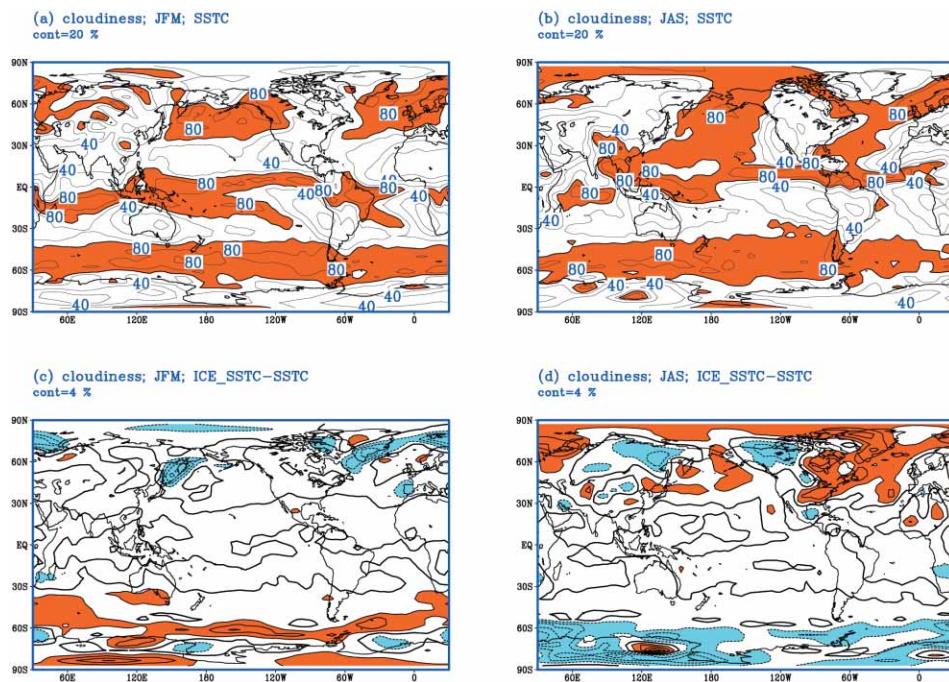


**Figure 6.** As Fig.2 but for total cloud cover. Cloudiness greater than 70% are shaded in a) and b). Contours every 20% in a) and b), and every 2% in c) and d).

Cloud difference fields reveal that some of largest variations in the cloud cover are found in the regions of seasonal sea-ice variability (Fig. 6c and 6d). In winter hemispheres, where the extent of sea ice is substantial, cloud cover is generally reduced in ICE\_SSTC with respect to climatological values defined by the control run. Thus, in the Northern Hemisphere, there is less clouds during JFM over the Arctic Ocean, the Greenland and Barents Seas and the Sea of Okhotsk; in the Southern Hemisphere, cloud cover is reduced alongside the southern sea-ice belt and over most of Antarctica. As mentioned above, a higher surface albedo over sea ice than over surrounding water decreases the incoming solar radiation and contributes to a further cooling of the surface. This cooling further stabilises already cold lower troposphere air through sinking motion and contributes to a reduction of the cloud amount. In addition, sea ice prevents evaporation from reaching the free atmosphere thus making less water vapour available for cloud formation processes.

In summer hemispheres, positive differences indicate an increased cloud cover in the regions where sea ice retracted. However, they also spread out further away from the regions of the maximum (winter) sea ice extension. This increased cloud amount could be linked to an increased ocean heat flux and associated evaporation that through conditional instability contribute to

increased convection in storm tracks. The increase of evaporation coincides with that of sensible heat flux (see the discussion for the temperature field above) reaching over  $5 \text{ mm day}^{-1}$  locally (not shown). A general warming of summer oceans contributes to more clouds in the northern Pacific and northern Atlantic where the proximity of warm continental surfaces contributes to a somewhat higher cloud increase than that found in the southern oceans, between  $30^\circ\text{S}$  and  $60^\circ\text{S}$ . In contrast, Royer et al. (1990) found unexpectedly a reduction in cloud cover over the ice-free Arctic; however, they attributed such a result to the parameterisation scheme for cumulus convection used in their model.

### *3.2. Zonally averaged vertical distributions*

In this subsection we examine the vertical extent of changes induced by the effect of the inter-experiment variations of sea ice. Because of predominantly large-scale nature of these changes, this is attained by analysing vertical cross sections for some zonally averaged thermodynamical fields. From the previous discussion some symmetry between hemispheres has been noticed; this is confirmed further in zonal averages.

The zonally averaged temperature distribution for JFM and JAS seasons in the control experiment (SSTC) is shown in Fig. 7a and 7b. When the thermodynamic effects of sea ice are included in the model, winter cooling and summer heating are found in the polar and subpolar regions of both hemispheres (cf. Figs. 2 and 3). Fig. 7c and 7d clearly shows that the impact of sea ice variation, in terms of ICE\_SSTC minus SSTC differences, is extended throughout the troposphere. However, whereas positive (summer) differences reach high levels, the negative ones are mostly confined to the lower and middle troposphere, in particular during the northern winter. For a given region, this indicates a relative weaker localised impact of the sea ice cooling in winter in comparison to a widespread warming due to the (sensible) heat flux from the ice-free ocean.

In both hemispheres, areas of positive (negative) temperature differences are associated with positive (negative) differences in geopotential height (Fig. 7e and 7f). The nearly zonally uniform seasonal variation of sea ice in the Southern Hemisphere causes variations in geopotential height that are almost identical in the amplitude and vertical extent but opposite in sign. In the Northern Hemisphere, the amplitude of positive differences in summer is twice as large as that of negative differences in winter, with both having maximum values located in the polar stratosphere. Such a seasonal asymmetry could be inferred to the zonally irregular land/sea distribution, as well as to zonally asymmetric differences in the spatial distribution of heat sources (for example, Fig. 1a indicates that the JFM sea-ice distribution in the northern Atlantic and the adjacent seas is largely governed by the northern extension of the Gulf Stream).

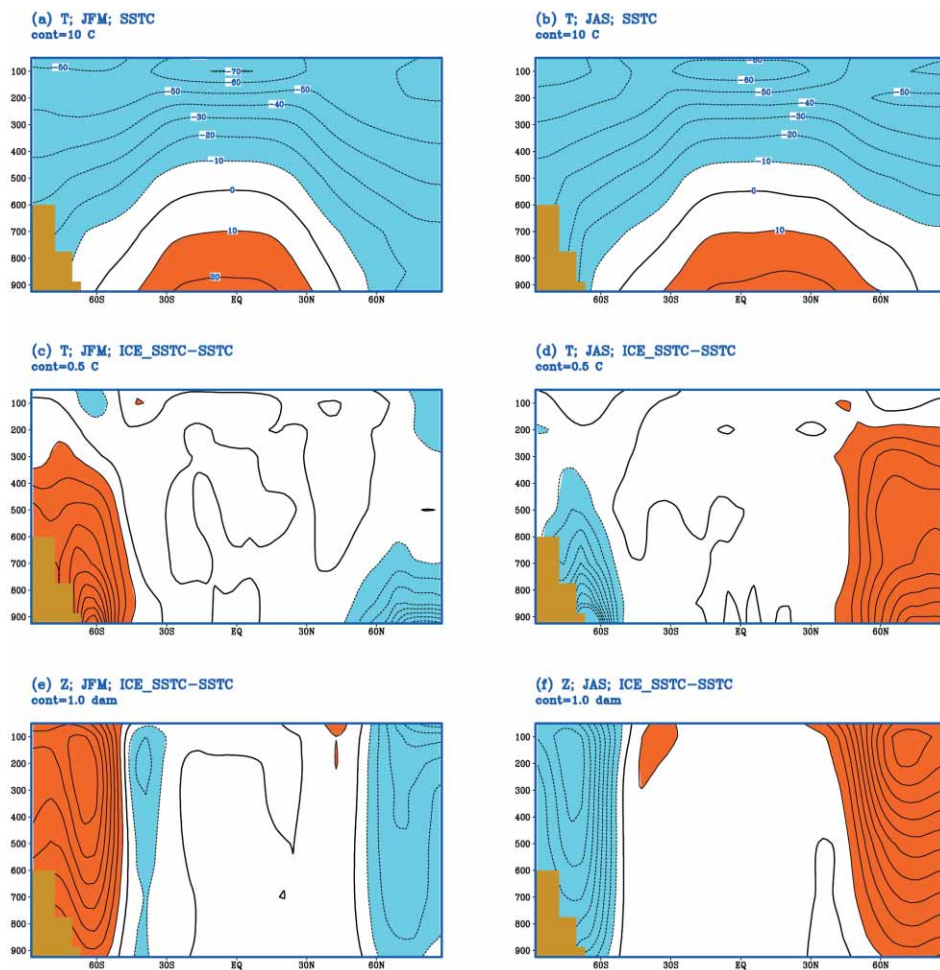


**Figure 7.** Zonally averaged cross sections for: a) temperature SSTC full field in JFM, b) temperature SSTC full field in JAS, c) temperature difference ICE\_SSTC minus SSTC in JFM, d) temperature difference ICE\_SSTC minus SSTC in JAS, e) geopotential height difference ICE\_SSTC minus SSTC in JFM, and f) geopotential height difference ICE\_SSTC minus SSTC in JAS. Contours every 10 °C in a) and b), every 0.5 °C in c) and d), and every 1 dam in e) and f). Shading as in Fig.2.

The zonally averaged  $u$ -wind shows that zonal circulation in both hemispheres is dominated by westerly jet maxima near 200 hPa (Fig. 8a and 8b). Some symmetry in the location of jet cores between the two hemispheres is seen: in winter hemispheres, the locations of jet cores are found at around 30°; in summer hemispheres, they are displaced poleward to between 40° and 45°. The amplitude of both winter and summer jets is larger in the Southern than in the Northern Hemisphere indicating that the wind drag, orographic friction

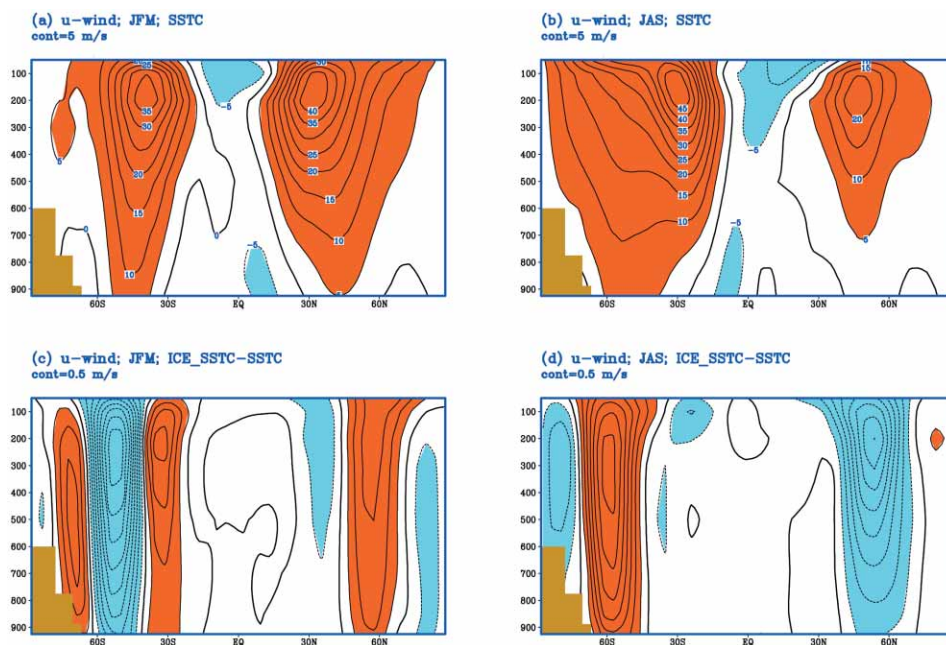


**Figure 8.** Zonally averaged cross sections for u-wind for: a) SSTC full field in JFM, b) SSTC full field in JAS, c) difference ICE\_SSTC minus SSTC in JFM, and d) difference ICE\_SSTC minus SSTC in JAS. Contours every  $5 \text{ ms}^{-1}$  in a) and b), and every  $0.5 \text{ ms}^{-1}$  in c) and d). Shading as in Fig. 2.

and the land/sea distribution in the Northern Hemisphere affect somewhat the average wind speed.

The differences ICE\_SSTC minus SSTC, indicating the impact of the sea-ice specification on zonal wind, are shown in Fig. 8c and 8d. Clearly, the changes introduced in ICE\_SSTC are felt throughout the vertical extent of the model atmosphere. In winter hemispheres (the Northern Hemisphere in Fig. 8c and the Southern Hemisphere in Fig. 8d), jet cores are slightly weakened, and the winds poleward of the jets are strengthened, suggesting a slight poleward shift of both winter jets. Royer et al. (1990) also found a poleward displacement of the westerly jet maximum during the winter season in the Northern Hemisphere. The wind strengthening in the Southern Hemisphere is approximately twice as large as in the Northern Hemisphere with the maximum at 300 hPa, *i.e.* at a somewhat lower level compared to the actual location of the southern jet core. As discussed above, this strengthening is related to the cooling of high latitudes imposed by the increased sea-ice cover (Fig. 7c and 7d), which is also evident in the decrease of geopotential heights (Fig. 7e and 7f). A relatively »deep« vertical extent of such a wind increase may be linked to the barotropic pattern of height differences that are, in turn, mainly governed by horizontal temperature differential gradients.

In summer, the increased ocean heat flux (in the absence of sea ice) tends to increase the vertical convective mixing, in particular in storm tracks, and to reduce  $u$ -wind accordingly. (In the Northern Hemisphere, this is also aided by an increased influence of orography on a generally weakened hemispheric circulation.) The regions of the maximum wind reduction are located poleward of seasonal jet cores implying an equatorward displacement of summer jets. Such a reduction is particularly discernible in the southern summer (Fig. 8c) where the equatorward shift of the jet core is also associated with an enhancement of  $u$ -wind around 30 °S. A strong temperature contrast between the largely ice-free Southern Ocean and cold Antarctica causes the stronger temperature gradient resulting in increased winds over Antarctica.

#### 4. Summary and conclusions

In this paper, the SPEEDY model was used to study the impact of climatological sea ice on the model atmosphere and the sensitivity of the atmospheric circulation to a different specification of sea-ice temperatures. Though SPEEDY is a model of intermediate complexity, it is able to reproduce reasonably well all the main features of climate and variability of the global circulation. The experimental set up consists of the two 50-year integrations: in the first, no thermodynamic effects of sea ice are included, and in the second, the computation of surface temperature over ice points takes into account contributions from various factors affecting the net heat flux into the surface. In both experiments climatological monthly mean SSTs are defined at the lower boundary. The seasonal mean difference between these two experiments is assumed to signify the thermodynamic impact of sea ice. This impact is assessed for two seasons, JFM and JAS, when in both hemispheres the sea-ice extension is at its extreme. Having only two long runs at our disposal forced with climatological data, it was assumed that relatively strong model internal variability (Bracco et al., 2004) may serve as a proxy for real (interannual) variability. With such an assumption, long runs with the recurrent climatological annual cycle could effectively represent ensembles of relatively shorter integrations and therefore give sufficient statistical weight to our results. It was demonstrated that, despite its relatively coarse horizontal and vertical resolutions, SPEEDY could reproduce the seasonally varying impact of sea ice on the global atmosphere, consistent with observational and other modelling studies.

The impact of a different specification of sea-ice temperatures in SPEEDY is mainly confined to high and mid latitudes with very little or no influence in the tropics. However, in the regions where such an impact exists, it generally extends throughout the depth of the model atmosphere revealing the barotropic characteristics of most of the changes. The inclusion of sea-ice temperatures determined by the SPEEDY thermodynamic model leads to the reduction of model temperatures during winter seasons in both hemispheres.

The strongest impact was found in the regions with the maximum sea-ice fraction (like, for example, the Sea of Okhotsk, the Greenland and Barents Seas in the Northern Hemisphere and along the land-sea boundary of Antarctica). Though the temperature response is found throughout the depth of the model atmosphere, it is strongest at low levels, weaker in the mid-troposphere, further weakened in the upper troposphere and completely lost in polar stratospheres. This sensitivity of the model temperature to the sea-ice forcing could be also viewed from a different perspective: our results clearly indicate that winters with the thermodynamic effect of sea ice are colder than winters when this effect is not included. Such a conclusion becomes relevant for a better understanding of the current climate change with the receding sea ice being one of the most dominant factors possibly influencing the future Earth climate.

In summer, when the sea-ice extent is much reduced or sea ice is completely absent (and in the Northern Hemisphere is also aided by the warming from the land surface), the opposite effect – a strong warming of the model atmosphere – is seen. The amplitude and the extent of summer warming is larger than those for winter cooling, indicating a stronger impact of ocean heat flux on the model atmosphere in comparison to that from sea ice.

The changes in geopotential heights generally follow those in temperature. In winter (summer) hemispheres, geopotential height decreases (increases) thus showing a direct relationship with the extent of sea ice. However, in contrast to temperature, geopotential height differences extend to the top of the model, having maxima at or near the tropopause. In addition, because of longitudinally quasi-uniform land/sea distribution, height differences in the Southern Hemisphere are more seasonally symmetric than their northern counterpart. Consistent with changes in geopotential height are the changes in zonal wind. The inclusion of the sea-ice thermodynamics leads to the strengthening (weakening) of zonal wind in the winter (summer) hemisphere throughout the model atmosphere. Such a relatively uniform vertical structure may be ultimately linked to a strong north–south (meridional) gradient in temperature differences, in particular in winter hemispheres, with no or very little vertical mixing. In addition, in the experiment with the sea-ice thermodynamics, jet cores are shifted poleward during the hemispheric winter, and slightly equatorward in summers.

As expected, the impact of sea ice (and of ice-free water) is also evident in the model distribution and amount of cloudiness. In winter, the impact over sea ice is conveyed through increased albedo and reduced solar radiation that stabilises lower troposphere by sinking motion, thus resulting in the reduced cloudiness. In summer, over the ice-free oceans, heat flux brings more moisture into the atmosphere and increases convective activity causing an increase in cloud cover.

Our results suggest that a general seasonally varying symmetry between the Northern and the Southern Hemispheres exists, in spite of their dif-

ferences in land/sea and, consequently, sea ice distribution. It is of interest to assess to what extent this hemispheric and seasonal quasi-symmetry will be disturbed when observed interannual variations in sea ice and/or SST are used instead of climatological fields. The results of such a study will be reported in due course.

*Acknowledgments* – We thank to Fred Kucharski and Franco Molteni from the Abdus Salam International Centre for Theoretical Physics (ICTP) in Trieste, Italy for the help in installing the SPEEDY model at the Geophysical Institute and for the comments and suggestions that improved this paper. The work of I. Herceg Bulić was supported by the Ministry of Science, Education and Sports of the Republic of Croatia under the Project no. 0119330.

## References

- Agnew, T. (1993): Simultaneous winter sea-ice and atmospheric circulation anomaly patterns. *Atmos. Ocean.*, **31**, 259–280.
- Alexander, M. A., Bhatt, U. S., Walsh, J. E., Timlin, M. S., Miller, J. S. and Scott, J. D. (2004): The atmospheric response to realistic Arctic sea ice anomalies in an AGCM during winter. *J. Climate*, **17**, 890–905.
- Bracco, A., Kucharski, F., Kallummal, R., and Molteni, F. (2004): Internal variability, external forcing and climate trends in multidecadal AGCM ensembles. *Climate Dynam.*, **23**, 659–678.
- Bourke, W. (1974): A multilevel spectral model. I. Formulation and hemispheric integrations. *Mon. Weather Rev.*, **102**, 687–701.
- Deser, C., Walsh, J. E. and Timlin, M. S. (2000): Arctic sea ice variability in the context of recent atmospheric circulation trends. *J. Climate*, **13**, 617–633.
- Fang, Z. and Wallace, J. M. (1994): Arctic sea ice variability on a timescale of weeks: Its relation to atmospheric forcing. *J. Climate*, **7**, 1897–1913.
- Gibson, J. K., Kallberg, P., Uppala, S., Hernandez, A., Nomura A. and Serrano, E. (1997): ECMWF reanalysis. Project report series. 1. ERA description. European Centre for Medium-Range Weather Forecasts, Reading (U.K)
- Gloersen, P. (1995): Modulation of sea ice cover by ENSO events. *Nature*, **373**, 503–506.
- Held, I. M. and Suarez, M. J. (1994): A proposal for the intercomparison of dynamical cores of atmospheric general circulation models. *B. Am. Meteorol. Soc.*, **75**, 1825–1830.
- Herman, G. F. and Johnson, W. T. (1978): The sensitivity of the general circulation to Arctic sea ice boundaries: A numerical experiment. *Mon. Weather Rev.* **106**, 1649–1664.
- Honda, M., Yamazaki, K., Tachibana, Y. and Takeuchi, K. (1996): Influence of Okhotsk Sea ice extent on the atmospheric circulation. *Geophys. Res. Lett.*, **23**, 3595–3598.
- Kahl, J. D. (1990): Characteristics of the low-level temperature inversion along the Alaska Arctic coast. *Int. J. Climatol.*, **10**, 537–548.
- Kalnay, E., Kanamitsu, M., Kistler, R., Collins, W., Deaven, D., Gandin, L., Iredell, M., Saha, S., White, G., Woollen, J., Zhu, Y., Chelliah, M., Ebisuzaki, W., Higgins, W., Janowiak, J., Mo, C., Ropelewski, C., Wang, J., Leetmaa, A., Reynolds, R., Jenne, R. and Joseph, D. (1996): The NCEP/NCAR 40-year reanalysis project. *B. Am. Meteorol. Soc.*, **77**, 437–471.
- Maslanik, J. A., Serreze, M. C. and Agnew, T. (1999): On the record reduction in 1998 western Arctic sea-ice cover. *Geophys. Res. Lett.*, **26**, 1905–1908.
- Mitchell, J. F. B. and Hills, T. S. (1986): Sea-ice and Antarctic winter circulation: A numerical experiment. *Q. J. Roy. Meteor. Soc.*, **112**, 953–969.

- Mitchell, J. F. B. and Senior, C. A. (1989): The Antarctic winter; simulations with climatological and reduced sea-ice extents. *Q. J. Roy. Meteor. Soc.*, **115**, 225–246.
- Molteni, F., Ferranti, L., Palmer, T. N. and Viterbo, P. (1993): A dynamical interpretation of the global response to equatorial Pacific SST anomalies. *J. Climate*, **6**, 777–795.
- Molteni, F. (2003): Atmospheric simulations using a GCM with simplified physical parameterizations. I: Model climatology and variability in multi-decadal experiments. *Climate Dynam.*, **20**, 175–191.
- Murray, R. J. and Simmonds, I. (1995): Responses of climate and cyclones to reductions in Arctic sea ice. *J. Geophys. Res.*, **100**, 4791–4806.
- Newson, R. L. (1973): Response of a general circulation model of the atmosphere to removal of the Arctic ice-cap, *Nature*, **241**, 39–40.
- Palmer, T. N. (1993): Extended-range atmospheric predictions and the Lorenz model. *B. Am. Meteorol. Soc.*, **74**, 49–65.
- Palmer, T. N. and Anderson, D. L. T. (1994): The prospects for seasonal forecasting – A review paper. *Q. J. Roy. Meteor. Soc.*, **120**, 755–793.
- Parkinson, C. L., Rind, D., Healy, R. J. and Martinson, D. G. (2001): The impact of sea ice concentration on climate model simulations with the GISS GCM. *J. Climate*, **14**, 2606–2623.
- Royer, J. F., Planton, S. and Déqué, M. (1990): A sensitivity experiment for the removal of Arctic sea ice with the French spectral general circulation model. *Climate Dynam.*, **5**, 1–17.
- Simmonds, I. and Budd, W. F. (1991): Sensitivity of the southern hemisphere circulation to leads in the Antarctic pack ice. *Q. J. Roy. Meteor. Soc.*, **113**, 1003–1024.
- Tjernström, M., Žagar, M., Svensson, G., Cassano, J. J., Pfeifer, S., Rinke, A., Wyser, K., Dethloff, K., Jones, C., Semmler, T. and Shaw, M. (2005): Modelling the Arctic boundary layer: An evaluation of six ARCMIP regional-scale models using data from the SHEBA project. *Bound.-Lay. Meteorol.*, **117**, 337–381.
- Warshaw, M. and Rapp, R. R. (1973): An experiment on the sensitivity of a global circulation model, *J. Appl. Meteorol.*, **12**, 43–49.
- Wu, B., Wang, J. and Walsh, J. (2004): Possible feedback of winter sea ice in the Greenland and Barents Seas on the local atmosphere. *Mon. Weather Rev.*, **132**, 1868–1876.

## SAŽETAK

**Utjecaj leda na površini mora na sezonske klimatske promjene**

*Ivana Herceg Bulić i Čedo Branković*

Utjecaj leda na površini mora na opću cirkulaciju atmosfere razmatran je pomoću relativno jednostavnog atmosferskog globalnog cirkulacijskog modela (nazvanog Speedy). Posebna je pažnja posvećena sezonskim promjenama raspodjele leda te njegovom termodinamičkom utjecaju. U tu su svrhu definirana dva eksperimenta: prvi koristi klimatološke mjesečne temperature leda na površini mora (dobivenih pomoću ERA-15 podataka), dok drugi eksperiment uključuje termodinamički model za dobivanje temperatura leda. U oba eksperimenta je integracija modelom izvedena u trajanju od 50 godina.

Rezultati pokazuju da termodinamički model pojačava sezonski ciklus temperature. Tako tijekom zime uključivanje termodinamičkog modela uzrokuje dodatno hlađenje atmosfere viših geografskih širina u odnosu na temperature dobivene integracijom modela s klimatološkim vrijednostima temperature leda na površini mora. Takva tempe-

ratorna raspodjela praćena je smanjenjem visina geopotencijalnih ploha te jaćanjem zonalnog vjetra. Također je modelom dobivena i smanjena naoblaka u području srednjih i viših geografskih širina. Hlađenje atmosfere može se izravno povezati sa sezonskim ciklusom jer led na površini mora povećava albedo te na taj način smanjuje upadno sunčevu zraćenje, a time dodatno stabilizira ionako hladni zrak. Neke od promjena uzrokovane ledom na površini mora se protežu kroz cijelu modeliranu atmosferu. Takvo ponašanje može se izravno povezati s jakim meridionalnim gradijentim temperature. Nadalje, uočena je određena sezonska simetrićnost između Sjeverne i Južne Hemisfere.

Tijekom ljeta kad je smanjen ledeni pokrov, model daje suprotne rezultate od onih dobivenih za zimsku sezonu: atmosfera je toplija uz slabljenje zonalnog vjetra i povećanu naoblaku. Ove promjene imaju veću amplitudu od onih povezanih s maksimalnom kolićinom ledenog pokrova tijekom zime. Taj rezultat upućuje na to da toplinski tokovi sa slobodne površine mora zajedno s povećanim sunčevim zraćenjem i konvekcijom imaju znaćajan utjecaj na modeliranu atmosferu.

*Ključne rijeći:* sezonska klimatska promjenjivost, termodinamićki utjecaj leda, model opće cirkulacije atmosfere

Corresponding author's address: Ivana Herceg Bulić, Department of Geophysics, Faculty of Science, University of Zagreb, 10000 Zagreb, Horvatovac b.b., Croatia, e-mail: iherceg@rudjer.irb.hr